11.5 ON THE RESPONSE OF HAILSTORMS TO ENHANCED CCN CONTRATIONS

Gustavo G. Carrió and William R. Cotton
Department of Atmospheric Science, Colorado State University, Fort Collins, Colorado

1. INTRODUCTION

This idealized study represents an exploration of the parameter space varying both CCN concentrations and cloud base heights. The analysis does not focus on the time evolution and behavior of individual hailstorms but it rather concentrates on a more macroscopic perspective, similar to that of recent study for orographic precipitation (Carrió and Cotton, 2013) or those for urban storms (Carrió et al, 2010; Carrió and Cotton, 2011; although varying cloud base heights instead of instability levels).

For this purpose, a three moment-scheme developed by Loftus (3MHAIL, 2013) was implemented into the Regional Atmospheric Modeling System (RAMS v. 6). This triple-moment bulk hail microphysics scheme predicts the relative dispersion parameter for a gamma distribution function via the prediction of the sixth moment (related to the reflectivity factor) of the distribution in addition to the mass mixing ratio and number concentration (third and zeroeth moments, respectively) thereby allowing for a fully prognostic distribution function.

The well-known narrowing of the hail size distributions as the precipitation core descends makes intuitive the limitations imposed by two-moment schemes that assume constant width parameters. Moreover, there is a significant improvement in the representation of sedimentation, melting, and formation processes of hail compared to lower-order moment schemes and previous versions of RAMS.

* *Corresponding author address:* Gustavo Gabriel Carrió, Department of Atmospheric Science, Colorado State University, Fort Collins, CO 80523; email: carrio@atmos.colostate.edu.

2. METHODOLOGY

2.1 *The Atmospheric Model*

The dynamical modeling framework used for this study is RAMS v. 6.0 (Pielke et al. 1992; Cotton et al. 2003). This non-hydrostatic model integrates predictive equations for the wind components, the Exner function, the ice-liquid water potential temperature, and the total mixing ratio on a vertically-stretched Arakawa C-grid.

In addition the recently implemented 3MHAIL modules, RAMS considers the explicit activation of CCN (and giant CCN), a bimodal representation of cloud droplets, and a bin-emulation approach for computing hydrometeor number concentration and mixing ratio changed due to all collisional mechanisms including droplet collection, and ice-particle riming (Saleeby and Cotton, 2004, 2008).

The mixing ratios and number concentrations of all water species (cloud droplets, drizzle drops, rain, pristine ice, snow, aggregates, graupel and hail) were predicted. CCN, GCCN and IFN concentrations were also considered as prognostic variables.

2.2 *Experimental Design*

RAMS was configured to cover an area 100x100km with 500m horizontal grid spacing (N_x=N_y=200) and a vertically-stretched grid (N_z=50) with the first model level at an altitude of approximately 40m. Potential CCN concentration was initialized by constant profiles below 3km and exponentially decreasing above.

A previously studied case (Loftus et al, 2013) was used as a benchmark to the experimental design of these set of cloud-

resolving simulations. The initial wind and thermodynamic profiles correspond to a hailstorm for which 1-inch diameter hail was reported (Figure 1). This vapor profile was systematically perturbed by modifying vapor contents at low levels; they were multiplied by factors between 0.85 and 1.15. These variations represent a displacement of approximately 500m in the cloud base altitude. Potential CCN concentrations were varied between 100 and 2400 cm^{-3} entering the domain.

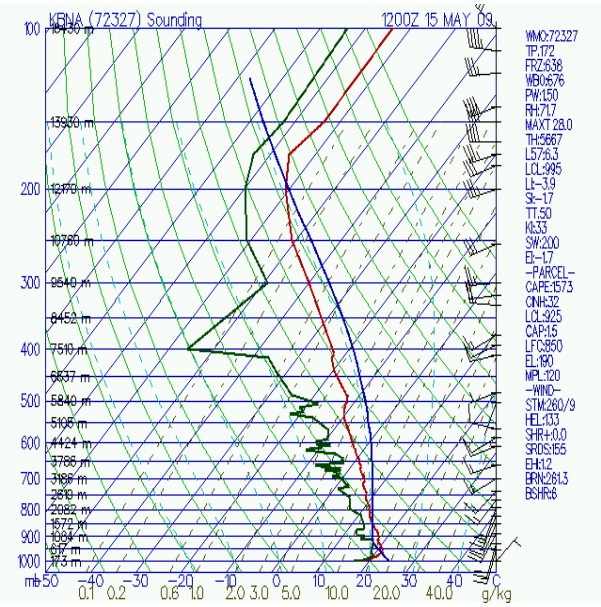

Figure 1 Benchmark soundings

All simulations were run for 90 minutes and initialized with a Gaussian bubble temperature perturbation. Its horizontal extent was 7km, a peak anomaly of 2.5K at 1000m, and it was located upwind from the domain center to ensure simulated hailstorms stayed far from the domain boundaries. Model output data were written every 3 minutes.

Figure 2 gives a schematic representation of the 160 numerical experiments. The x-axis varies entering potential CCN concentrations, the blue arrow denotes runs for the cleanest air mass, and the y-axis enhancements of low-level vapor content with respect to the profile of the benchmark case. The green arrow denotes runs that ingest the original soundings.

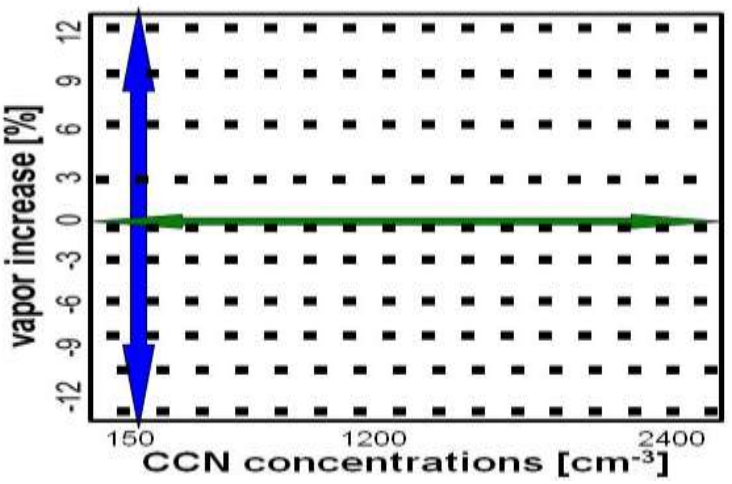

Figure 2 Experimental design.

3. RESULTS

Naturally more moist runs (lower cloud base temperatures) generated more intense updrafts (greater CAPE), however, increasing potential CCN concentrations had lesser impact on the moist simulations compared to the drier runs (higher cloud base temperatures), as seen in Figure 3.

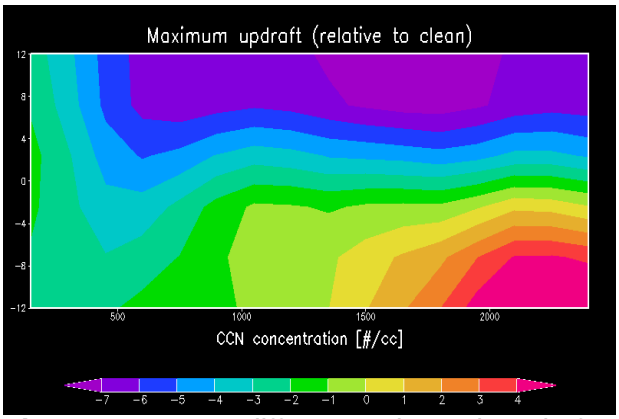

Figure 3. Percent differences in peak updrafts relative to the clean case for each low-level moisture level. Y-axis gives percent change in low-level vapor contents. Zero represents the benchmark case.

Figure 3 shows the difference in maximum updraft (relative to that of the cleanest runs for

all low-level vapor contents between 88 and 112% of the benchmark case. A relative increase (up to 5%) can be seen when increasing CCN concentrations, mainly for cases with vapor contents lower than the benchmark case.

A similar behavior has been observed for the integral mass of hail precipitation (Fig 4) that is mainly dominated by the availability of water vapor. However, for vapor anomalies less than +6%, a monotonic increase in potential CCN concentrations relative to the "clean" case (corresponding to each vapor level) shows a monotonic increase in total mass of hail precipitation (see Fig. 5). A very similar behavior can be observed in Figure 6 that shows the ratio between the total mass of precipitation and the integral cloud base upwelling vapor flux.

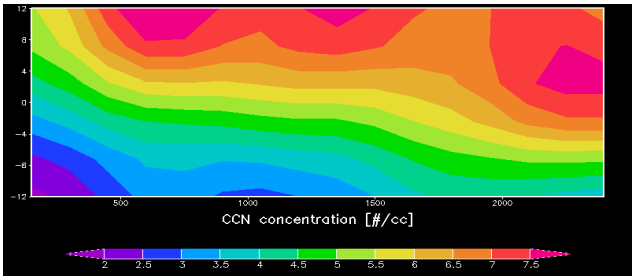

Figure 4 Integral mass of hail precipitation Y-axis gives percent change in low-level vapor contents and zero is the benchmark case. Shaded areas represent mass (X 10^6 kg).

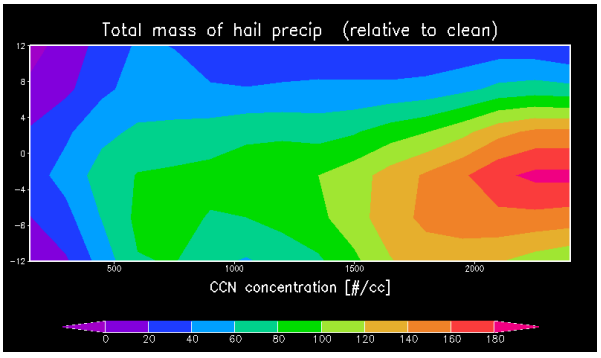

Figure 5 Same as Figure 8 but for percent differences in the total mass of hail precipitation relative to the clean case for each low-level moisture level. Shaded areas represent percent differences.

The diameters corresponding to mass-weighted hailstone volume (predominant diameters) are compared in Figure 7. The response tends to be monotonic when potential CCN concentration is increased, with weaker response for drier environments. However, the peak hailstone number concentration (areal) tended to monotonically increase with CCN concentrations for drier cases (not shown).

Peak integral conversion rates from supercooled liquid (SCLW) to hail are compared in absolute values and relative to each corresponding clean case in Figs 8 and 9, respectively. The absolute values of these peak rates are mainly governed by the low-level vapor contents; however, again, a clear monotonic decrease is visible for the wetter cases (Fig. 8).

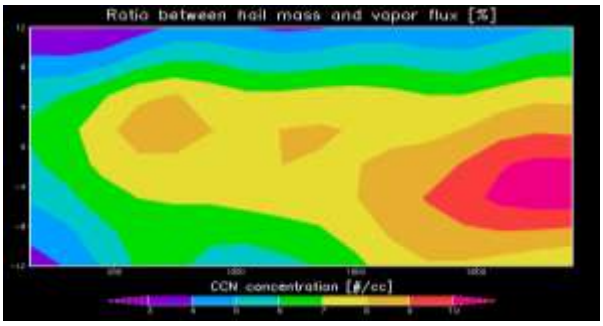

Figure 6. Overall mass ratios between hail precipitation and vapor processes by the storm [%].

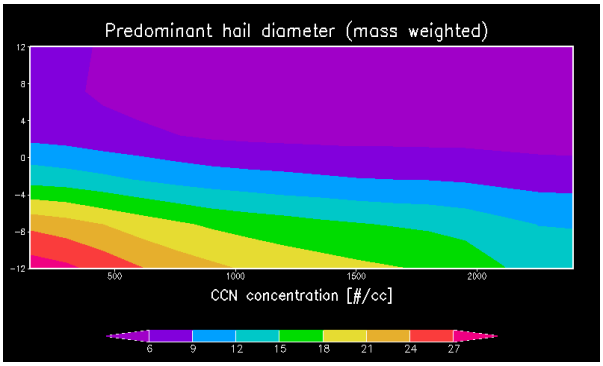

Figure 7. Predominant hail diameters [mm].

Precipitation loading at the time of maximum updraft strength shows a similar behavior (not shown). In terms of relative changes, the response for drier cases when increasing

CCN concentrations is not regular although positive differences prevail (Fig 9). Only negative changes with decreases were seen for the wetter cases.

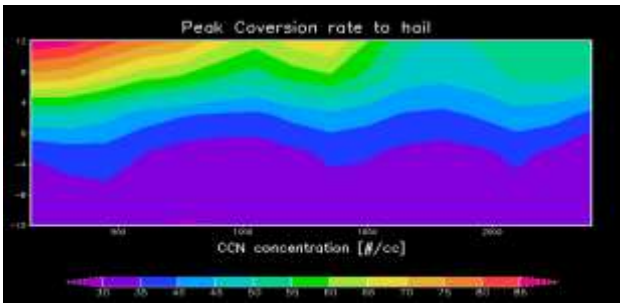

Figure 8. Peak conversion rates from supercooled liquid to hail [kg X 10^6 s^{-1}].

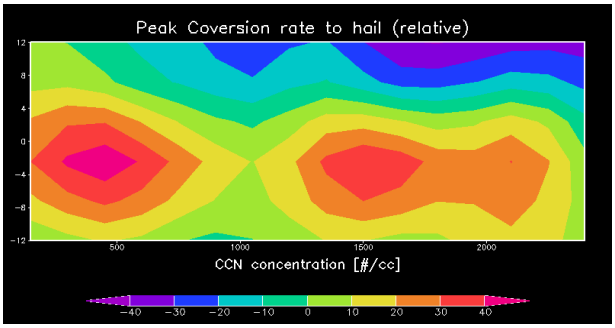

Figure 9. Idem Figure 8 but in this case, shaded areas represent percent differences with respect to the corresponding clean case.

More intense updrafts appear to cover smaller areas generating larger (local) hail accumulations (Figure 10).

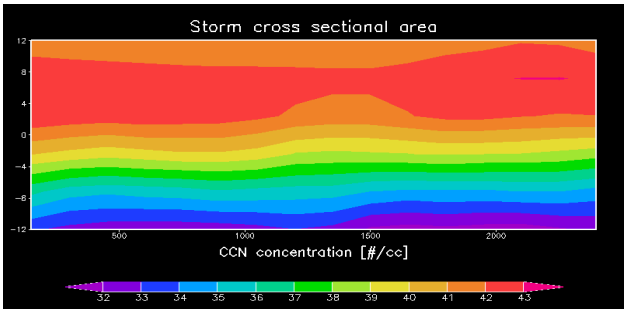

Figure 10 Comparison of areas with positive hail precipitation rates at the time the maximum (local) hail precipitation rates occurs.

A representative "storm size" in Figure 10 is given in Km as a diameter, assuming a circular shape of the aforementioned area.

Finally, the peak mass of hail integrated over the cloud is dominated by the availability of supercooled liquid water (SCLW), and also linked to the response of maximum updrafts.

The response of the integral mass and the peak SCLW content are compared in Figure 11. Both quantities show a very similar behavior that is also analogous to that of maximum updraft (see Fig 3). When increasing CCN concentrations, important increases are seen for those runs with higher cloud base. Conversely, a weaker dependence is seen for the runs with a deeper layer between cloud base and the freezing level.

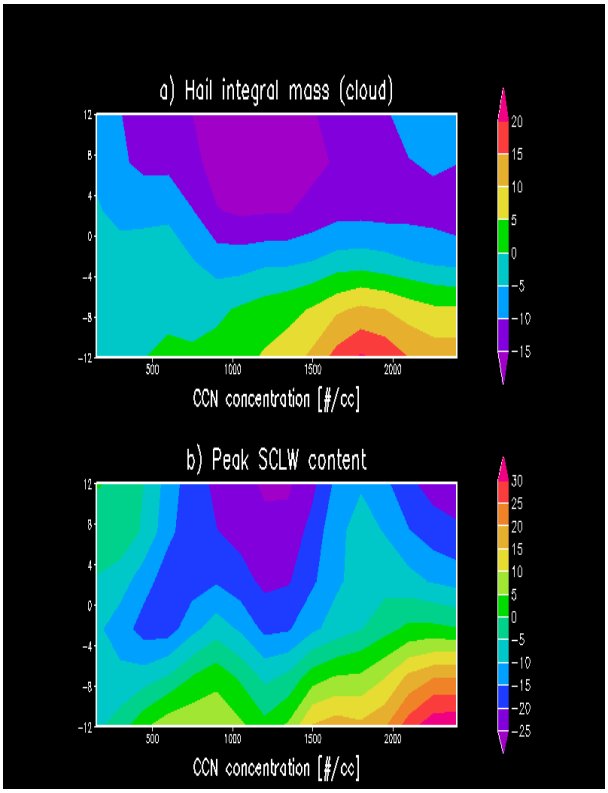

Figure 11. In-cloud integral mass of hail and SCLW content, both compares as peak values normalized by the clean case. Shaded areas represent percent differences with respect to the clean case.

4. CONCLUSIONS

We performed a rather large number of hailstorm simulations exploring the parameter space to examine the CCN-effect dependence on environmental factors (i.e., cloud base). A previously studied hailstorm case was used as a benchmark, and low-level vapor contents were systematically varied.

As naturally expected, for experiments with lower cloud base temperature (greater CAPE)more intense storms were simulated; however, enhancing CCN concentrations exhibited a greater impact on the moist simulations compared to the drier runs. Simulated maximum accumulations and integral masses of hail precipitation, and hail predominant sizes are especially affected for the "drier" runs.

The depth of the layer between cloud base and the freezing level is connected to higher instabilities and higher updrafts. INvreasing the depth of the aforementioned layer implicitly increases the formation of warm rain and, on the other hand, the higher updrafts "dilute" the microphysical effects (i.e., cloud droplet size reduction) leading to weaker enhancements in SCLW. These results are consistent with previous studies (Carrió et al 2010; Carrió and Cotton, 2011).

Results also suggest that the areas with hail precipitation (when the maximum precipitation rates occur) for drier cases tend to be slightly lower when CCN concentrations increase, (also seen by Carrió and Cotton, 2011). We are currently using numerous post-processing codes to compare several other aspects such as morphological changes (e.g., cross sectional areas of the updrafts the peak values are achieved, downdrafts, cold pools, etc).

5. ACKNOWLEDGEMENTS

The authors wish to thank the National Science Foundation (NSF) for financial support (AGS-1005041).

6. REFERENCES

Carrió, G.G. and W.R. Cotton: Theoretical exploration of cloud-nucleating aerosol conditions that could allow snowfall enhancement over the Sierra Nevada. *Submitted to Atmospheric Research.*

Carrió G.G., Cotton, W. R., 2011: Effects of the Urban growth of Houston on convection and precipitation. Part II: Their dependence on instability. Atmospheric Research, 102, 167-174.

Carrió G.G, Cotton, W. R., Cheng, 2010: Effects of the Urban growth of Houston on convection and precipitation. Part I: the August 2000 case. Atmospheric Research, 96, 560-574.

Cotton, W. R., R. A. Pielke Sr., R. L. Walko, G. E. Liston, C. J. Tremback, H. Jiang, R.L. McAnelly, J.Y. Harrington, M. E. Nicholls, G. G. Carrio, and J. P. McFadden, 2003: Rams 2001: Current status and future directions. *Meteor. Atmos. Phys.*, 82, 5-29.

Loftus, A.M., Cotton, W. R. and G. G. Carrió, 2013: CCN Impacts on Hail. Part I: Description and Initial Evaluation of a Triple-Moment Hail Bulk Microphysics Scheme. *Submitted to Journal of the Atmospheric*.

Pielke, R. A., and Coauthors, 1992: A comprehensive meteorological modeling system- RAMS. *Meteor. Atmos. Phys.*, 49, 69-91.

Saleeby, S. M., and W.R. Cotton, 2008: A Binned Approach to Cloud-Droplet Riming Implemented in a Bulk Microphysics Model. *J. Appl. Meteo,* 47, 694-703.

Saleeby, S. M., and W.R. Cotton, 2004: A large-droplet model and prognostic number concentration of cloud droplets in the RAMS@CSU model. Part I: Module descriptions and Supercell test simulations. *J. Appl. Meteo,* 43, 182-195.